Platinum-graphene counter electrodes for dye-sensitized solar cells

Cheng-En Cheng, Chi-Yuan Lin, Chien-Hsun Shan, Shang-Yi Tsai, Ko-Wei Lin, Chen-Shiung Chang, and Forest Shih-Sen Chien

Citation: Journal of Applied Physics **114**, 014503 (2013); doi: 10.1063/1.4812498
View online: http://dx.doi.org/10.1063/1.4812498
View Table of Contents: http://scitation.aip.org/content/aip/journal/jap/114/1?ver=pdfcov
Published by the AIP Publishing

Platinum-graphene counter electrodes for dye-sensitized solar cells

Cheng-En Cheng,[1,2] Chi-Yuan Lin,[1,2] Chien-Hsun Shan,[3] Shang-Yi Tsai,[2] Ko-Wei Lin,[2] Chen-Shiung Chang,[1,3] and Forest Shih-Sen Chien[2,4,a)]

[1]*Department of Photonics and Institute of Electro-Optical Engineering, National Chiao Tung University, Hsinchu 30010, Taiwan*
[2]*Department of Physics, Tunghai University, Taichung 40704, Taiwan*
[3]*Department of Photonics and Institute of Display, National Chiao Tung University, Hsinchu 30010, Taiwan*
[4]*Tunghai Green Energy Development and Management Institute, Tunghai University, Taichung 40704, Taiwan*

(Received 23 March 2013; accepted 13 June 2013; published online 2 July 2013)

This paper describes the photovoltaic performance of dye-sensitized solar cells (DSSCs) containing graphene-incorporated counter electrodes (CEs). The location and thickness of graphene in CEs are optimized to improve the photovoltaic performance of DSSCs, compared with typical Pt CEs. The DSSC, with a Pt/few-layer graphene (FLG) CE, achieved 8% in short-circuit current density and 13% in power conversion efficiency (PCE). Electrochemical impedance spectroscopy shows that the DSSC, with a Pt/FLG CE, exhibits a series resistance lower than that with a Pt CE. The lower series resistance is attributed to the contact resistance at the interface of platinum and fluorine doped tin oxide. The contact resistance is reduced by the formation of the thin platinum-carbon composite layer. It is demonstrated that the consumption of Pt could be reduced with a Pt/FLG CE. However, graphene/Pt CEs resulted in a slow charge-transfer process and consequently a worse photovoltaic performance of DSSCs. © *2013 AIP Publishing LLC*. [http://dx.doi.org/10.1063/1.4812498]

I. INTRODUCTION

In the field of sustainable green energy, dye-sensitized solar cells (DSSCs) have attracted much interest. Many advantages are provided by DSSCs: low cost, simplicity of preparation, and high conversion efficiency.[1] A typical DSSC includes a dye-sensitized photo-anode, a redox electrolyte, and a counter electrode (CE). The function of the CE is to catalyze the redox couple regeneration and collect electrons.[2,3] Pt is suitable for use in CEs because of its high catalytic activity during the reduction of I_3^-. However, the noble metal Pt is rare and expensive. Therefore, reducing the consumption of Pt is an important consideration for the wide deployment of DSSCs.

Graphene has unique optical and electrical properties[4,5] and has been employed in the CEs of DSSCs. For example, graphene has been used in DSSCs to provide electrochemically stable CEs with I_3^-/I^--based electrolyte[6] and $Co(bpy)_3^{3+/2+}$ -based electrolyte.[7] The enhanced performance of DSSCs with metal-graphene composite CEs has been demonstrated in previous studies. Examples of these composites include $Ni_{12}P_5$/graphene oxide[8] and Ni/graphene.[9] Bajpai *et al*. reported that the performance of DSSCs was enhanced by graphene-supported Pt nanoparticle CEs.[10] Therefore, graphene-incorporated CEs could be good candidates for reducing the consumption of Pt in DSSCs.

This study presents the effectiveness of graphene-incorporated CEs for DSSCs. The location and thickness of the graphene in CEs were studied to improve the energy-conversion performance of DSSCs and reduce the amount of Pt used. Two locations of graphene are used in the examined CEs: (1) The interface between Pt and fluorine doped tin oxide (FTO) to provide better contact at the Pt/FTO junction and (2) the interface of the Pt/electrolyte to improve the electrocatalytic ability of the device. Fig. 1 shows these CEs with different sequences of graphene and Pt layers employed in this study: (1) Pt over graphene (Pt/graphene) and (2) graphene over Pt (graphene/Pt). Few-layer graphene (FLG) and multilayer graphene (MLG) were considered in this research. With Pt/FLG CEs, enhancements of 8% in the short-circuit current density (J_{sc}) and 12.5% in the power conversion efficiency (PCE) were achieved. The application of FLG at the interface between Pt and FTO reduced the contact resistance by 21%, which was derived by electrochemical impedance spectroscopy (EIS). The depth profile of Auger electron spectroscopy (AES) indicated the existence of a thin platinum-carbon composite between Pt and FTO. The thin Pt-C composite resulted in better contact between Pt and FTO, and the photocurrent was raised. The Pt/FLG CE can reduce the consumption of Pt by 75%. However, the graphene/Pt CEs did not improve the electrocatalytic ability and photovoltaic performance at all.

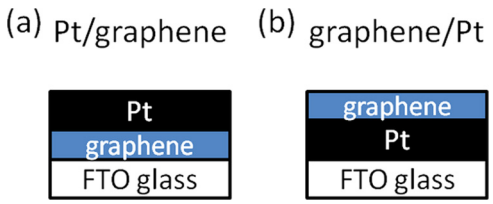

FIG. 1. Two schematics of graphene-incorporated CEs for DSSCs: (a) the Pt/graphene CEs and (b) the graphene/Pt CEs.

a)Author to whom correspondence should be addressed. Electronic mail: fsschien@thu.edu.tw.

II. EXPERIMENTAL

The graphene layers were grown by chemical vapor deposition (CVD). A 1 cm^2 Cu foil was placed in a quartz furnace and heated to 1050 °C (for FLG) and 1000 °C (for MLG) for 30 min., with a N_2 gas flow and an alkane source. Epitaxial graphene was transferred[11] on FTO glass. The number of layers was 1–2 for FLG or 10–12 for MLG, respectively, which were verified by transmission spectroscopy[12] (Hitachi 3300 UV-Vis spectrometer) and confocal Raman spectroscopy with a 633 nm He-Ne laser, as shown in Fig. 2. A sputtered-Pt layer for electrocatalysis, electric contact, and light reflection was deposited over and under the transferred graphene for Pt/graphene and graphene/Pt CEs, respectively (Fig. 1). A Pt/FTO CE was prepared as a reference.

For the fabrication of DSSCs, the photo-anodes were prepared with the following steps: (1) P25 TiO_2 paste was spin-coated on FTO glass with an area of 0.64 cm^2 and a thickness of 10 μm; (2) the P25 TiO_2 film was sintered at 400 °C in air for 30 min to create porous structures; and (3) the porous P25 TiO_2 film was soaked in a 0.3 mM solution of ruthenium dye N719 in anhydrous ethanol for 14 h. Finally, the photo-anode and CE were assembled with a 60 μm spacer in a sandwich type, in which the electrolyte was filled. The electrolyte was prepared by 0.5 M KI and 0.05 M I_2 in propylene carbonate. The current density-voltage (J–V) characteristics of the DSSCs were recorded on a current-voltage source meter under the illumination of a xenon light source with an AM1.5G filter. The EIS of the DSSCs were examined in the frequency range of 1 Hz to 100 kHz by using a LCR meter (HIOKI 3522-50 LCR HiTESTER). The chemical composition of the Pt/graphene CE was analyzed by AES to study the properties of the junctions.

III. RESULTS AND DISCUSSION

A. DSSCs with Pt/graphene CEs

The J–V characteristic curves of DSSCs with Pt/graphene CEs and a reference DSSC with Pt CE are shown in Fig. 3. The sputtered-Pt layers are 200 nm thick. The photovoltaic parameters from the J–V curves are summarized in Table I. The J_{sc} and PCE of these devices are 16.0 mA/cm^2 and 5.6% (Pt), 17.3 mA/cm^2 and 6.3% (Pt/FLG), and 11.4 mA/cm^2 and 4.4% (Pt/MLG), respectively. The DSSC with Pt/FLG CE outperformed the reference device by 8%

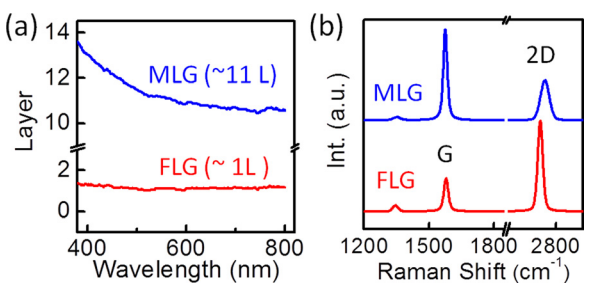

FIG. 2. (a) Number of layers = [1-T(λ)]/0.023 derived from the transmittance spectra T(λ) of FLG and MLG to show that FLG is 1–2 layers and MLG is 10–12 layers, where λ is the wavelength and 0.023 corresponds to the attenuation of one graphene layer, and (b) Raman spectra of FLG and MLG. The high ratio of 2D band to G band of FLG shows it is only 1 or 2 layers.

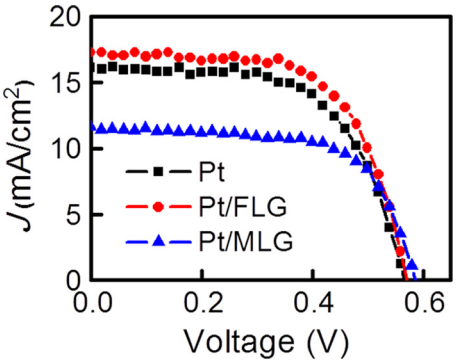

FIG. 3. J–V characteristic curves of DSSCs with Pt (reference), Pt/FLG, and Pt/MLG CEs.

and 12.5% in J_{sc} and PCE, respectively. The improvement in J_{sc} was achieved by reducing the contact resistance of Pt/FLG CEs, which is explained later with the result of EIS. Furthermore, these DSSCs had a similar open-circuit voltage (V_{oc}) and filling factor (FF), that is, 559 mV and 63% (Pt), 559 mV and 64% (Pt/FLG), and 579 mV and 67% (Pt/MLG), respectively. These results indicate that the Pt/graphene CEs have no influence on V_{oc} and FF.

In general, DSSCs can be represented by an equivalent circuit, as shown in Fig. 4(a). From the Nyquist plot of complex impedance of DSSCs, the series resistance (R_s) describes the bulk resistance,[9] including the resistances of electrodes, electrolyte, and contact. The radius of the semicircle in the high-frequency region (>100 Hz) is the charge-transfer resistance (R_{ct}), associated to electrocatalytic reactions of Pt and I_3^-.[3,13] The radius of the semicircle in the mid-frequency region (10 to 100 Hz) is the recombination resistance (R_{rec}), related to the injected electron transport process at the interfaces of TiO_2/electrolyte and TiO_2/dye.[14,15] The low-frequency region (<10 Hz) represents the Nernst diffusion process of I^- and I_3^- within the spacer.[9,16] The EIS of DSSCs with Pt/graphene CEs was taken under illumination to identify the electrochemical behaviors shown in Fig. 4(b). The impedance spectra were simulated in the frequency region of 1 Hz to 100 kHz with the Z-view software by the equivalent circuit shown in Fig. 4(a). The details of the simulated results are summarized in Table I. The signal in the low-frequency region (<1 Hz) was omitted because it represents the electrolyte diffusion process within the spacer, which was not altered in the study.

The R_s in DSSCs with various CEs is 3.3 Ω (Pt), 2.7 Ω (Pt/FLG), and 5.3 Ω (Pt/MLG), respectively. The DSSC with a Pt/FLG CE had an R_s lower than that of a reference DSSC.

TABLE I. Photovoltaic parameters of DSSCs with different counter electrodes, from J–V measurement and the simulated resistances from EIS.

	J–V				EIS		
Electrode	J_{sc} (mA/cm^2)	V_{oc} (mV)	FF (%)	PCE (%)	R_s (Ω)	R_{ct} (Ω)	R_{rec} (Ω)
Pt	16.0	559	63	5.6	3.3	12	129
Pt/FLG	17.3	559	64	6.3	2.7	12	131
Pt/MLG	11.4	579	67	4.4	5.3	18	132

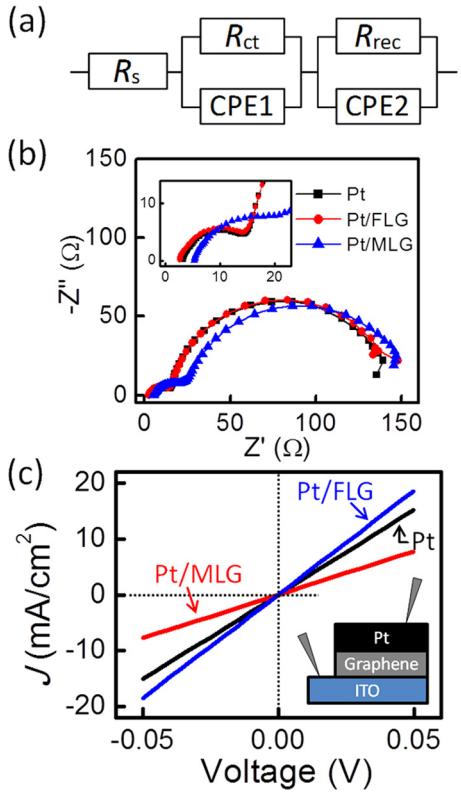

FIG. 4. (a) Equivalent circuit of the DSSCs. (b) Complex impedance Nyquist plots of DSSCs with Pt (reference), Pt/FLG, and Pt/MLG CEs from EIS. The EIS was taken with a frequency range of 1 Hz to 100 kHz under illumination. The enlarged plots of the high-frequency regime are inset into (b). (c) The *J*–*V* curves of Pt/graphene/ITO. A *J*–*V* curve of Pt/ITO without graphene is also given as a reference. The inset in (c) presents the schematic of Pt/graphene/ITO.

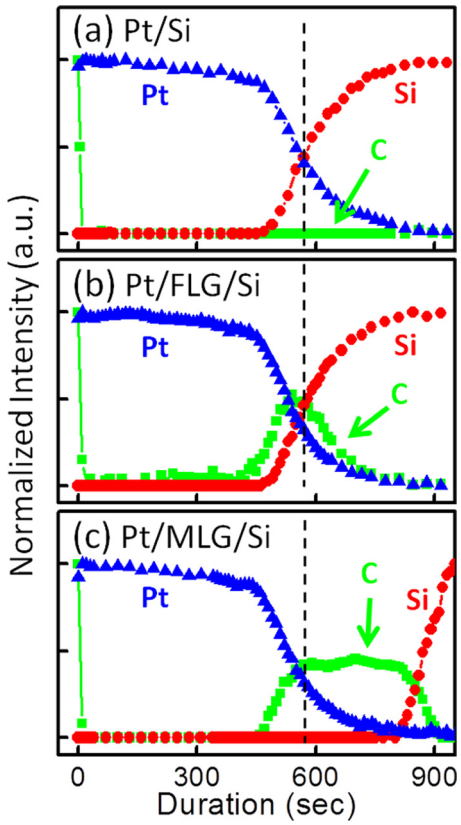

FIG. 5. AES depth analyses of Pt (MNN), C (KLL), and Si (LMM) of the Pt/Si (a), Pt/FLG/Si (b), and Pt/MLG/Si (c), respectively. The dashed line discloses the interface of Pt/Si in (a) and (b), and Pt/C in (c), respectively.

These measurements indicate that FLG changed the contact resistance of the Pt/FTO junction and further increased the photocurrent and efficiency. However, a Pt/MLG CE resulted in a worse R_s. To verify that the contact resistance of the Pt/FTO junction was reduced by FLG, the contact resistance of the Pt/FLG/ITO and Pt/MLG/ITO was measured, as shown in the inset of Fig. 4(c) (ITO stands for indium tin oxide, which is also employed as a CE substrate[17,18]). The junction area is approximately 9 mm^2. The *J*–*V* curves of Pt/FLG/ITO and Pt/MLG/ITO are shown in Fig. 4(c), and that of Pt/ITO is also presented as a reference. All of these contacts exhibited the ohmic behavior shown in the *J*–*V* curves. Clearly, the Pt/FLG/ITO exhibits the lowest contact resistance, and the Pt/MLG/ITO exhibits a worse contact resistance than the reference of Pt/ITO, which is consistent with the results of EIS. The FLG reduced R_s by lowering the contact resistance of the Pt-FTO junction. Accordingly, the J_{sc} and PCE of DSSCs with Pt/FLG CE were improved. However, MLG did not have a similar effect on DSSCs.

The interfacial property of Pt/graphene was studied by AES depth analyses. The Pt/graphene was prepared on Si substrates to avoid charging effects during AES measurement. A uniform 25 mm^2 graphene film was transferred onto the Si substrate and was subjected to the deposition of a 50 nm layer of Pt by DC sputtering. The intensities of Auger electrons were recorded at the peaks of Pt MNN (1961 eV), C KLL (266 eV), and Si KLL (1616 eV). Fig. 5(a) shows that the reference Pt/Si had a sharp interface, and no C signal was detected. For Pt/FLG/Si, the distributions of Pt and Si were the same as that of Pt/Si [Fig. 5(b)]. In addition, the C peak was observed at the junction of Pt and Si, indicating the location of graphene. The graphene was suspected to have suffered from a defect-inducing process during the sputtering of Pt. The graphene was attacked by the plasma and Pt atoms and became reactive to form an interfacial Pt-C composite at the junction of Pt/Si. The thin interfacial Pt-C composite, because of FLG, was thought to reduce the contact resistance of the metal-semiconductor junction of Pt and FTO. From the AES depth profile of Pt/MLG/Si [Fig. 5(c)], the distributions of Pt and Si were similar to those of Pt/Si and Pt/FLG/Si. A thin Pt-C composite was also formed at the Pt/MLG/Si junction, but a thicker C (actually several nanometers only) existed at the junction. However, the MLG is so thick that the whole graphene did not become a Pt-C composite. The perpendicular charge transportation of the residual graphene layer is poor, leading to a higher contact resistance at the junction of Pt/FTO and a lower photocurrent in the photovoltaic performance of Pt/MLG CE.

The charge-transfer resistance (R_{ct}) in DSSCs is 12 Ω for both Pt and Pt/FLG, and 18 Ω for Pt/MLG, respectively. The Pt/graphene CEs did not improve the electrocatalytic ability of DSSCs. This indicates that the increase in photocurrent with the Pt/FLG CE was not due to a faster charge-transfer process at the electrolyte/Pt interface. However, R_{rec}

is associated with the electron recombination rate in DSSCs and is 129 Ω (Pt), 131 Ω (Pt/FLG), and 132 Ω (Pt/MLG), respectively. This suggests that a similar charge recombination process occurred in DSSCs with Pt/graphene and Pt CEs, which accounts for the same V_{oc} in photovoltaic performance.

The efficiency of Pt/FLG CEs provides an opportunity to reduce the consumption of Pt. Two additional CEs, with a lower loading of Pt (50 nm Pt and 50 nm Pt/FLG), were prepared to demonstrate the possibility. The *J–V* characteristic curves and the Nyquist plots of DSSCs with Pt (200 nm), Pt (50 nm), and Pt (50 nm)/FLG CEs are shown in Fig. 6. The photovoltaic parameters from *J–V* measurement and resistances in the equivalent circuit from EIS are summarized in Table II. Compared with the DSSC with a Pt (200 nm) CE, the DSSC with Pt (50 nm) CE shows a lower J_{sc} and higher R_{ct}, which indicates that the decrease in J_{sc} may be attributed to the thinner Pt. The thicker Pt (200 nm) provides a higher charge-transfer ability because its R_{ct} is lower. The reason for the dependence of the charge-transfer ability on the Pt thickness is unclear. The DSSC with a Pt (50 nm)/FLG CE presents photovoltaic performance similar to that of DSSCs with Pt (200 nm) CE. Hence, the cost of a lower charge-transfer ability with thinner Pt (50 nm) was balanced out by the lower R_s of Pt (50 nm)/FLG.

B. DSSCs with graphene/Pt CEs

Graphene has been reported to be good in electrocatalysis.[19] Therefore, graphene/Pt CEs might be able to improve the electrocatalytic reaction in DSSCs. The photovoltaic *J–V* characteristic curves of DSSCs with Pt (reference), FLG/Pt, and MLG/Pt CEs are shown in Fig. 7(a). The sputtered-Pt layers are 200 nm thick. All photovoltaic parameters are summarized in Table III. The corresponding J_{sc} and PCE of DSSCs with graphene/Pt CEs were observed to be 14.9 mA/cm^2 and 3.8% (FLG/Pt), and 13 mA/cm^2 and 3.3% (MLG/Pt), respectively. The DSSCs with graphene/Pt CEs had poor performance in J_{sc} and PCE. Moreover, the V_{oc} and FF of the DSSCs exhibited 519 mV and 50% with FLG/Pt CEs, and 519 mV and 48% with MLG/Pt CEs, respectively. The poor FF and V_{oc} indicate that graphene/Pt CEs resulted in a higher charge recombination rate.

The resistances in the equivalent circuit of DSSCs with graphene/Pt CEs are derived from the Nyquist plot of complex impedance [shown in Fig. 7(b)] and are summarized in Table III. The R_s and R_{ct} are as follows: 4.8 Ω and 68 Ω (FLG/Pt), and 4.5 Ω and 63 Ω (MLG/Pt), respectively. Compared with the reference DSSC, both the R_s and R_{ct} of DSSCs with graphene/Pt CEs were increased. The decrease in J_{sc} appears to result from the higher R_s and worse

TABLE II. Photovoltaic parameters of DSSCs with different counter electrodes, from *J–V* measurement and the simulated resistances from EIS.

	J–V				EIS		
Electrode	J_{sc} (mA/cm^2)	V_{oc} (mV)	FF (%)	PCE (%)	R_s (Ω)	R_{ct} (Ω)	R_{rec} (Ω)
Pt[a]	16.0	559	63	5.6	3.3	12	129
Pt[b]	14.0	559	63	4.9	3.2	15	127
Pt/FLG[b]	16.5	559	63	5.7	2.8	15	128

[a]The thickness of the Pt layer is 200 nm and the parameters are from the reference device with a Pt CE in Table I.
[b]The thickness of the Pt layer is 50 nm.

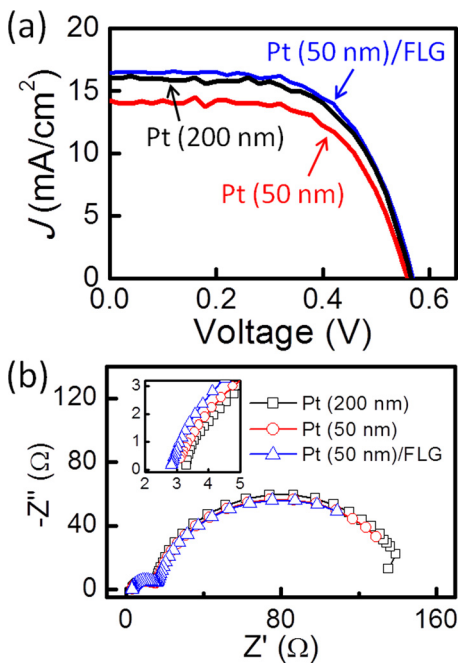

FIG. 6. (a) *J–V* characteristic curves and (b) Nyquist plots of DSSCs with Pt (200 nm), Pt (50 nm), and Pt (50 nm)/FLG CEs. The plots of complex impedance of these devices are similar. The significant difference is in R_s, as in the inset of (b), the enlarged plot of the low impedance part.

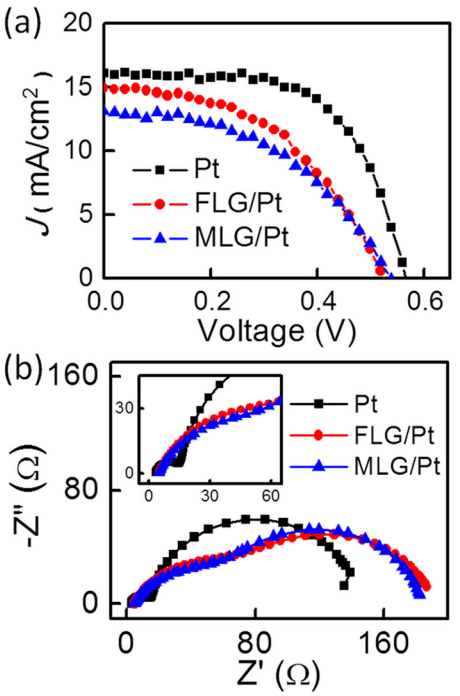

FIG. 7. *J–V* characteristic curves (a) and Nyquist plots of the complex impedance (b) of DSSCs with Pt (reference), FLG/Pt, and MLG/Pt CEs. The EIS was taken with a frequency range of 1 Hz to 100 kHz under illumination.

TABLE III. Photovoltaic parameters of DSSCs with different counter electrodes, from *J–V* measurement and the simulated resistances from EIS.

	J–V				EIS		
Electrode	J_{sc} (mA/cm^2)	V_{oc} (mV)	FF (%)	PCE (%)	R_s (Ω)	R_{ct} (Ω)	R_{rec} (Ω)
Pt[a]	16.0	559	63	5.6	3.3	12	129
FLG/Pt	14.9	519	50	3.8	4.8	68	119
MLG/Pt	13.0	519	48	3.3	4.5	63	116

[a]The parameters are from the reference device with a Pt CE in Table I.

electrocatalytic ability of graphene/Pt CEs. Graphene/Pt CEs do not behave according to study expectations, which are that the electrocatalytic reaction would be improved by graphene at the interface of Pt and electrolyte. Furthermore, the EIS presented R_{rec} of 119 Ω and 116 Ω with FLG/Pt CE and MLG/Pt CE, respectively. In the DSSCs with graphene/Pt CEs, the lower R_{rec} indicated that more charge recombination occurred at the interface of TiO_2/electrolyte.[15,16] This study suggests that the lower electrocatalytic ability with graphene/Pt CEs causes an increase in the concentration of I_3^- in electrolyte and leads to an increase of the recombination rate at the interface of TiO_2/electrolyte. Consequentially, both the worse R_{ct} and R_{rec} reflect the significantly low PCE of DSSCs with graphene/Pt CEs.

IV. CONCLUSION

This article reports that the photovoltaic performance of DSSCs improved with graphene-incorporated CEs, as the location and thickness of graphene were optimized. The DSSC with Pt/FLG CE was shown to provide 8% and 13% enhancement in J_{sc} and PCE, respectively. The results from EIS indicate that the increase of J_{sc} is attributed to the reduction of contact resistance of Pt-FTO, caused by the Pt-C composite. This approach can also be applied to junction modifications of metal-semiconductor interfaces, to reduce the contact loss. Based on this approach, the consumption of Pt can be reduced by 75%. This study also reports that the graphene/Pt CEs for DSSCs reduced the charge-transfer ability and lowered the photovoltaic performance.

ACKNOWLEDGMENTS

This work was supported by National Science Council, Taiwan and the Project of Global Research & Education on Environment and Society, Tunghai University.

[1]B. O'Regan and M. Gratzal, Nature **353**, 737 (1991).
[2]A. Kay and M. Gratzel, Sol. Energy Mater. Sol. Cells **44**, 99 (1996).
[3]Q. W. Jiang, G. R. Li, and X. P. Gao, Chem. Commun. **0**, 6720 (2009).
[4]A. K. Geim and K. S. Novoselov, Nature Mater. **6**, 183 (2007).
[5]Y. Zhu, S. Murali, W. Cai, X. Li, J. W. Suk, J. R. Potts, and R. S. Ruoff, Adv. Mater. **22**, 3906 (2010).
[6]L. Kavan, J. H. Yum, and M. Gratzel, ACS Nano **5**, 165 (2011).
[7]L. Kavan, J. H. Yum, and M. Gratzel, Nano Lett. **11**, 5501 (2011).
[8]Y. Y. Dou, G. R. Li, J. Song, and X. P. Gao, Phys. Chem. Chem. Phys. **14**, 1339 (2012).
[9]R. Bajpai, S. Roy, N. Kulshrestha, J. Rafiee, N. Koratkar, and D. S. Misra, Nanoscale **4**, 926 (2012).
[10]R. Bajpai, S. Roy, P. Kumar, P. Bajpai, N. Kulshrestha, J. Rafiee, N. Koratkar, and D. S. Misra, ACS Appl. Mater. Interfaces **3**, 3884 (2011).
[11]K. S. Kim, Y. Zhao, H. Jang, S. Y. Lee, J. M. Kim, K. S. Kim, J. H. Ahn, P. Kim, J.-Y. Choi, and B. H. Hong, Nature **457**, 706 (2009).
[12]R. R. Nair, P. Blake, A. N. Grigorenko, K. S. Novoselov, T. J. Booth, T. Stauber, N. M. R. Peres, and A. K. Geim, Science **320**, 1308 (2008).
[13]G.-R. Li, F. Wang, Q.-W. Jiang, X.-P. Gao, and P.-W. Shen, Angew. Chem. Int. Ed. **49**, 3653 (2010).
[14]Y. J. Chang and T. J. Chow, J. Mater. Chem. **21**, 9523 (2011).
[15]N. Cho, H. Choi, D. Kim, K. Song, M. S. Kang, S. O. Kang, and J. Ko, Tetrahedron **65**, 6236 (2009).
[16]E. Ramasamy, W. J. Lee, D. Y. Lee, and J. S. Song, Electrochem. Commun. **10**, 1087 (2008).
[17]W. Hong, Y. Xu, G. Lu, C. Li, and G. Shi, Electrochem. Commun. **10**, 1555 (2008).
[18]S. Ito, N.-L. C. Ha, G. Rothenberger, P. Liska, P. Comte, S. M. Zakeeruddin, P. Pechy, M. K. Nazeeruddin, and M. Gratzel, Chem. Commun. **38**, 4004 (2006).
[19]L. Qu, Y. Liu, J.-B. Baek, and L. Dai, ACS Nano **4**, 1321 (2010).